JACS
JOURNAL OF THE AMERICAN CHEMICAL SOCIETY
pubs.acs.org/JACS
Article

A Transient Iron Carbide Generated by Cyaphide Cleavage

Duleeka C. Wannipurage, Eric S. Yang, Austin D. Chivington, Jess Fletcher, Debanik Ray, Nobuyuki Yamamoto, Maren Pink, Jose M. Goicoechea,* and Jeremy M. Smith*

Cite This: J. Am. Chem. Soc. 2024, 146, 27173−27178
Read Online
ACCESS | Metrics & More | Article Recommendations | Supporting Information

ABSTRACT: Despite their potential relevance as molecular models for industrial and biological catalysis, well-defined mononuclear iron carbide complexes are unknown, in part due to the limited number of appropriate C_1 synthons. Here, we show the ability of the cyaphide anion ($C{\equiv}P^-$) to serve as a C_1 source. The high spin (S = 2) cyaphide complex PhB(^{t}BuIm)$_3$Fe−C≡P (PhB(^{t}BuIm)$_3^-$ = phenyl(tris(3-*tert*-butylimidazol-2-ylidene)borate) is readily accessed using the new cyaphide transfer reagent [Mg(^{Dipp}NacNac)-(CP)]$_2$ (^{Dipp}NacNac = CH{C(CH$_3$)N(Dipp)}$_2$ and Dipp = 2,6-di(iso-propyl)phenyl). Phosphorus atom abstraction is effected by the three-coordinate Mo(III) complex Mo(N^{t}BuAr)$_3$ (Ar = 3,5-Me$_2$C$_6$H$_3$), which produces the known phosphide (^{t}BuArN)$_3$Mo≡P along with a transient iron carbide complex PhB(^{t}BuIm)$_3$Fe≡C. Electronic structure calculations reveal that PhB(^{t}BuIm)$_3$Fe≡C adopts a doublet ground state with nonzero spin density on the carbide ligand. While isolation of this complex is thwarted by rapid dimerization to afford the corresponding diiron ethynediyl complex, the carbide can be intercepted by styrene to provide an iron alkylidene.

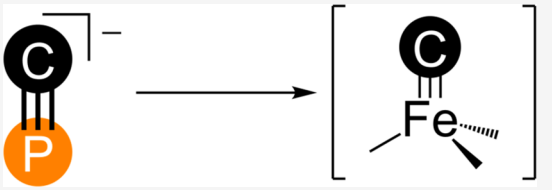

INTRODUCTION

Transition metal carbides (formally C^{4-}) are integral to the development of alternative energy sources.[1] For example, oxygenated feedstocks such as biomass, organic waste, coal, and natural gas are a source of synthesis gas (CO and H_2) that is subsequently converted to a mixture of hydrocarbons by the Fischer−Tropsch (F-T) CO hydrogenation process.[2] Mechanistically, heterogeneous F-T catalysts (typically Fe, Co, Ni, Ru) are proposed to cleave the strong C≡O bond to provide surface carbides[3] that are precursors to the C−C bond forming steps.[2,4] Transition metal carbides are also relevant in biology, most notably as interstitial atoms in the active site clusters of the nitrogenase enzymes, FeMoco[5] and FeVco.[6] Isotopic labeling and crystallographic studies have led to the suggestion that the carbide ligands provide structural integrity,[7] although they have also been proposed to play an electronic role by facilitating the delocalization of electron density.[8]

Well-defined model complexes can provide insight into the properties of the [M≡C] unit, however only a handful of terminal carbide complexes are known (Figure 1, top) This rarity is due in large part to the limited scope of known synthetic routes.[9] While multiple strategies toward metal carbide complexes have been reported, all have significant limitations that limit more widespread adoption. The most common strategy for installing terminal carbides involves C≡E bond cleavage of carbonyl and thiocarbonyl ligands.[10−12] Indeed, the carbide ligand in the first reported example, [(^{t}BuArN)$_3$Mo≡C]$^-$ (Ar = 3,5-Me$_2$C$_6$H$_3$), was sourced from carbon monoxide.[10] Bond cleavage reactions of other C_1 ligands (e.g., halocarbynes) have also been used to prepare other terminal carbides.[13] However, the specific challenges associated with these C_1 sources limit their general applicability.[14]

An alternate synthetic strategy involves carbon atom transfer from an appropriate reagent (Figure 1, bottom). These reagents are driven by the formation of highly stable product(s). While there are a small number of agents for C_1 transfer,[15] including to transition metal ions, the challenges associated with each of these compounds limits their more general use.[16]

To date, complexes with terminal carbide ligands are restricted to 4d and 5d transition metal ions, with no examples for any 3d metal ion.[9] Despite theoretical predictions suggesting the stability of terminal iron carbides,[17] attempts to deoxygenate or desulfurize C≡O and C≡S ligands in iron complexes have so far been unsuccessful.[18] The limited number of synthetic routes hinders access to terminal iron carbide complexes.

Inspired by the recent developments in cyaphide ($C{\equiv}P^-$) chemistry,[19] we hypothesized that this anion could serve as a convenient synthon for the carbide ligand. Importantly for its deployment as a C_1 source, the bond strength of cyaphide is lower than that of C≡O, and new transfer agents make its complexes more accessible than those of C≡S.

Received: August 5, 2024
Revised: September 5, 2024
Accepted: September 6, 2024
Published: September 17, 2024

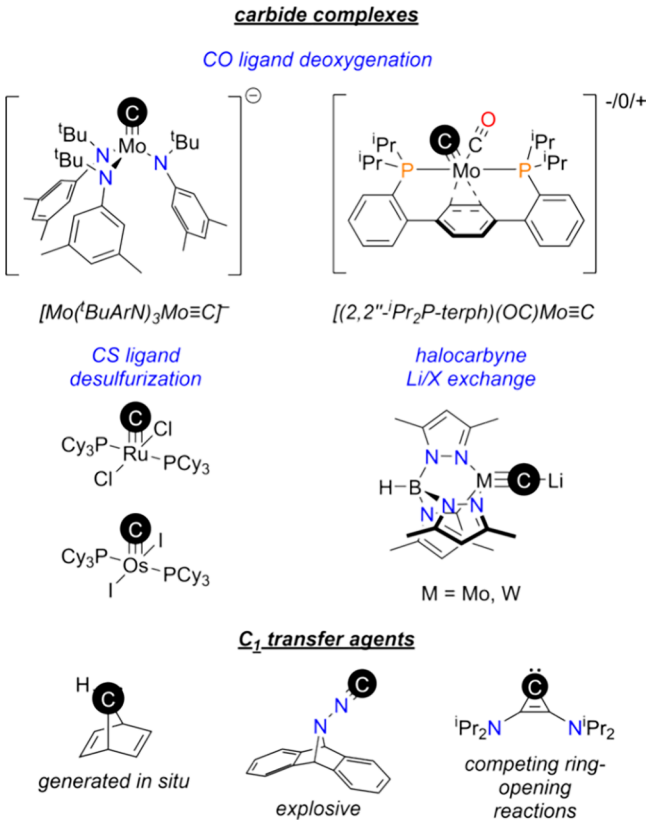

Figure 1. Top: Transition metal complexes with terminal carbide ligands, along with the source of the carbide ligand. Bottom: Examples of carbon atom transfer reagents.

We have demonstrated the utility of bulky tris(carbene)-borates as a platform for stabilizing multiply bonded atomic ligands on iron, with examples of isolable nitrido,[20] oxo[21] and sulfido[22] complexes. As part of these studies, we targeted a reductive cleavage strategy for accessing a carbide ligand, where a synthetic roadmap is provided by the assembly of $PhB(^{t}BuIm)_3Fe{=}N{=}C{=}Mo(N^{t}BuAr)_3$ from $PhB(^{t}BuIm)_3Fe{-}C{\equiv}N$ and $Mo(N^{t}BuAr)_3$.[23] While the proclivity of the cyaphide ligand to bridge metals through a $\mu{-}\eta^1{:}\eta^2$-C≡P coordination mode is a potential challenge to this strategy,[19] we anticipated that bulky supporting ligands would favor the $\eta^1{:}\eta^1$ mode as a precursor to cleavage.

RESULTS AND DISCUSSION

The use of *in situ* generated $Mg(^{Dipp}NacNac)(CP)(dioxane)$ as a cyaphide transfer reagent ($^{Dipp}NacNac$ = $CH\{C(CH_3)N(Dipp)\}_2$ and Dipp = 2,6-di(iso-propyl)phenyl) has previously been reported.[24a] While operationally simple, this protocol is not without its limitations; the *in situ* generation of the $^{i}Pr_3SiOCP$ precursor can only be done in benzene or toluene, and its reduction results in the presence of equimolar quantities of a siloxymagnesium byproduct which often complicates product isolation. We have found that performing the reduction in the absence of coordinating solvents results in the formation of a solvent-free dimer with bridging cyaphide ions, $[Mg(^{Dipp}NacNac)(CP)]_2$ (**Mg_{CP}**; see the Supporting Information for details). **Mg_{CP}** has drastically reduced solubility compared to its solvent adducts, allowing facile isolation on gram scale in good yields. The addition of Lewis bases (whether equimolar or in excess) results in quantitative conversion to previously reported hydrocarbon-soluble solvent adducts.

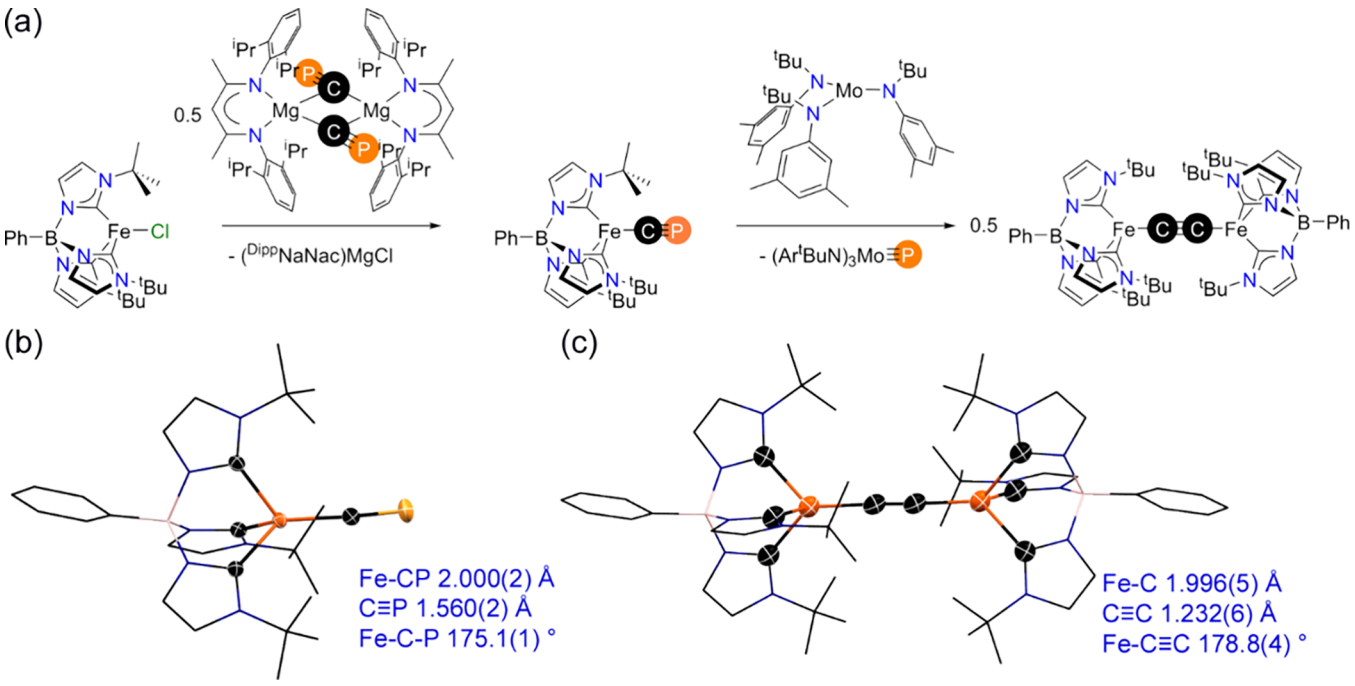

Figure 2. (a) Synthetic scheme leading to cyaphide ligand cleavage in an iron(II) complex. X-ray crystal structures of (b) $PhB(^{t}BuIm)_3Fe{-}C{\equiv}P$ and (c) $PhB(^{t}BuIm)_3Fe{-}C{\equiv}C{-}Fe(^{t}BuIm)_3BPh$ along with selected bond lengths (Å) and angles (deg). Thermal ellipsoids are shown at 50%, probability, hydrogen atoms omitted and most of the tris(carbene)borate ligand shown as wireframe for clarity. Black, orange and gold ellipsoids represent carbon, iron, and phosphorus atoms, respectively.

https://doi.org/10.1021/jacs.4c10704
J. Am. Chem. Soc. 2024, 146, 27173−27178

This new cyaphide transfer reagent reacts cleanly with PhB(^{t}BuIm)$_3$FeCl to afford the four-coordinate high spin (S = 2) complex PhB(^{t}BuIm)$_3$Fe−C≡P in high yield (Figure 2a), which has been fully characterized, including by single crystal X-ray diffraction (Figure 2b). To the best of our knowledge, this is the first example of a paramagnetic transition metal cyaphide complex.[25] Nonetheless, the structural (C≡P 1.560(2) Å) and spectroscopic (ν_{CP} = 1265 cm^{-1} by Raman spectroscopy) metrics of the cyaphide ligand are comparable with those observed in diamagnetic complexes.[24] The zero-field ^{57}Fe Mössbauer spectral parameters (δ = 0.42 mm/s, ΔE_Q = 1.21 mm/s) are similar to those reported for related iron(II) tris(carbene)borate complexes.[26]

At room temperature, PhB(^{t}BuIm)$_3$Fe−C≡P rapidly reacts with equimolar Mo(N^{t}BuAr)$_3$ (Ar = 3,5-Me$_2$C$_6$H$_3$)[27] to quantitatively afford (^{t}BuArN)$_3$Mo≡P[28] and the diiron μ_2-ethynediyl complex, PhB(^{t}BuIm)$_3$Fe−C≡C−Fe(^{t}BuIm)$_3$BPh (Figure 2a).[29] The diiron complex has been structurally (Figure 2c) and spectroscopically characterized (C≡C 1.232(6) Å, ν_{CC} = 1872 cm^{-1} by Raman spectroscopy). These metrics are most consistent with two high spin (S = 2) iron centers linked by a μ−η^1:η^1-C_2^{2-} ligand, which is also supported by the zero-field ^{57}Fe Mössbauer spectral parameters (δ = 0.45 mm/s, ΔE_Q = 0.84 mm/s).

Mechanistically, phosphorus atom abstraction from PhB(^{t}BuIm)$_3$Fe−C≡P implicates formation of the terminal carbide complex PhB(^{t}BuIm)$_3$Fe≡C that undergoes rapid C−C coupling to afford the diiron ethynediyl product. Electronic structure calculations provide insight into the nature of the carbide complex, PhB(^{t}BuIm)$_3$Fe≡C. A doublet (S = 1/2) ground spin state is favored by DFT calculations for a range of functionals. The optimized structure reveals a C_s-symmetric complex in which the four-coordinate iron center is bound to the tris(carbene)borate and carbide ligands. The very short Fe≡C bond (1.521 Å) is consistent with considerable iron−carbon multiple bond character. This distance is at least about 0.1 Å shorter than in crystallographically characterized diiron carbide-bridged complexes.[30] As with the isoelectronic iron(V) nitride complex, [PhB(^{t}BuIm)$_3$Fe≡N]$^+$,[31] which also has a doublet group spin state, PhB(^{t}BuIm)$_3$Fe≡C is distorted from C_{3v} symmetry. Notably, the B−Fe≡C angle (173.6°) is bent, while two longer (2.019 Å, 2.012 Å) and one shorter tris(carbene)borate Fe−C distance (1.966 Å) is observed. This distortion likely arises from a pseudo Jahn−Teller distortion, as observed for [PhB(^{t}BuIm)$_3$Fe≡N]$^+$.[31]

The doublet ground state is also supported by CASSCF/NEVPT2 calculations. To a first approximation, the dominant configuration (75%) of the doublet state, as determined by CASSCF(9,8) calculations for PhB(^{t}BuIm)$_3$Fe≡C, corresponds to a (d_{xy}, $d_{x^2-y^2}$)^2(d_{z^2})^1(d_{xz}, d_{yz}) configuration (z axis along the B−Fe vector) of a formally Fe(V) center. Although weighted toward the iron center, the σ- and π-bonding SOMO − 4 and SOMO − 5 orbitals have a large degree of covalency. The metal based SOMO and SOMO − 1 orbitals are largely nonbonding (Figure 3, Figure S35). No Fe−C antibonding orbitals are occupied, suggesting an iron−carbon triple bond. This is consistent with NBO calculations[32] that reveal a covalent Fe≡C bond composed of one σ and two π-bonds (Table S4).

The CASSCF(9,8) calculations also reveal configurations (10% total) containing a triplet carbide ligand (Figure S54). These configurations transfer non-negligible spin density to the carbide ligand (Löwdin spin density = 0.22). These triplet

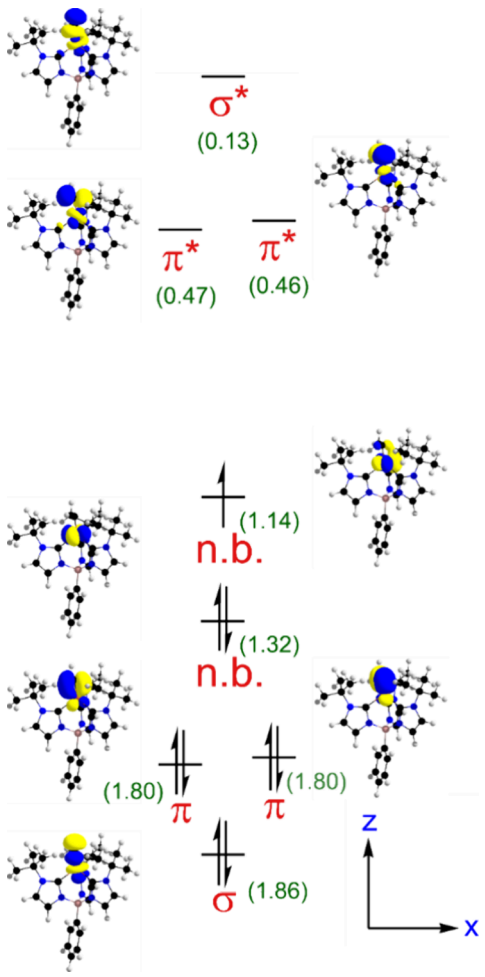

Figure 3. Dominant electronic configuration for PhB(^{t}BuIm)$_3$Fe≡C (S = 1/2), as determined by CASSCF(9,8) calculations. Total electron occupancy for each orbital shown in green and Fe−C orbital interactions indicated in red. Isodensity 0.05.

resonances also enable facile ethynediyl formation via a radical coupling mechanism. Similar carbide radical character is observed in the reduced complex [(2,2″-^{i}Pr$_2$P-terph)(OC)-Mo≡C]$^-$, which likewise undergoes C−C bond coupling.[33]

Monitoring the reaction between PhB(^{t}BuIm)$_3$Fe−C≡P and Mo(N^{t}BuAr)$_3$ by low temperature UV−vis spectroscopy provides spectral evidence for a reaction intermediate. Specifically, at −60 °C we observe the reversible formation of a red species with bands at 485, 525, and 725 nm. These bands are tentatively assigned to the cyaphide-bridged complex PhB(^{t}BuIm)$_3$Fe-CP-Mo(N^{t}BuAr)$_3$, akin to our previously reported complex PhB(^{t}BuIm)$_3$Fe═N═C═Mo(N^{t}BuAr)$_3$.[34] Importantly, none of the reagents, products, or potential side products (e.g., Mo(^{t}BuArN)$_3$═N═N═Mo(N^{t}BuAr)$_3$,[35] which is formed by reaction of Mo(N^{t}BuAr)$_3$ with N$_2$) have bands at these wavelengths. Variable temperature UV−vis spectroscopy reveals that this complex is in equilibrium with PhB(^{t}BuIm)$_3$Fe−C≡P and Mo(N^{t}BuAr)$_3$, with estimated ΔH = 1.4 kcal/mol and ΔS = −7.0 e.u. ($\Delta G \approx 0$ kcal/mol at −60 °C). At temperatures above ca. − 30 °C, irreversible bleaching of the bands is observed, which we attribute to cyaphide ligand cleavage.

Attempts to trap PhB(^{t}BuIm)$_3$Fe≡C are hindered by the facile formation of the ethynediyl product as well as the

https://doi.org/10.1021/jacs.4c10704
J. Am. Chem. Soc. 2024, 146, 27173−27178

reactivity of $Mo(N^tBuAr)_3$ toward common trapping agents (e.g., CO). Nonetheless, in an initial result, we have found that the carbide ligand can be intercepted by an activated alkene. Specifically, conducting the reaction of $PhB(^tBuIm)_3Fe{-}C{\equiv}P$ with $Mo(N^tBuAr)_3$ in the presence of excess styrene yields the iron cyclopropylidene complex $PhB(^tBuIm)_3Fe(C_3H_3Ph)$ as the major iron-containing product (Figure 4a). The ethyndiyl complex $PhB(^tBuIm)_3Fe{-}C{\equiv}C{-}Fe(^tBuIm)_3BPh$ accounts for the balance of the iron-containing material.

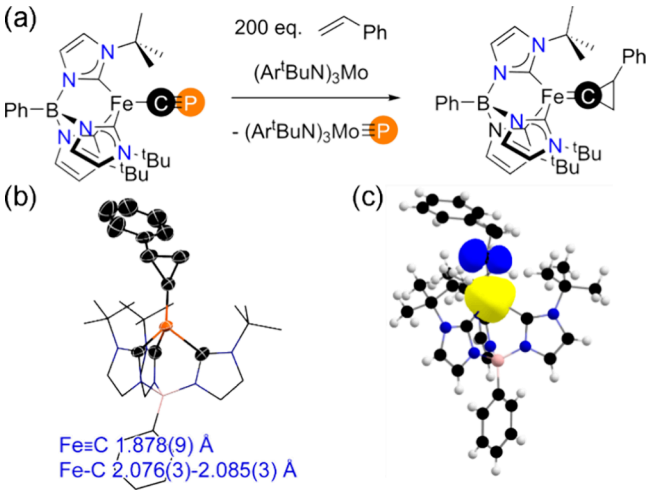

Figure 4. Synthesis and characterization of $PhB(^tBuIm)_3Fe(C_3H_3Ph)$. (a) Styrene traps an iron(V) carbide to provide an alkylidene complex; (b) X-ray crystal structure with selected bond lengths (Å) and angles (deg).Thermal ellipsoids are shown at 50% probability, hydrogen atoms and disorder omitted for clarity. Most of the tris(carbene)borate ligand shown as wireframe. Black and orange ellipsoids represent carbon and iron atoms, respectively; (c) spin density as determined by a CASSCF(7,6) calculation. Isodensity 0.001.

The molecular structure of $PhB(^tBuIm)_3Fe(C_3H_3Ph)$ reveals a four-coordinate iron center with a short Fe=C bond (1.878(9) Å) to the cyclopropylidene ligand. This bond length is shorter than is observed in the open shell iron alkylidene complexes (calix[4]-arene)Fe=CPh_2 (1.946(8) Å)[36] and (^{Et}PDI)Fe=CPh_2 (1.936(2) Å),[37] but similar to that observed in (^{Mes}PDPPh)Fe=CPh_2 (1.850(2) Å).[38] All three C−C bond lengths of the cyclopropylidene ligand are similar (1.530(18)−1.558(14) Å), excluding the possibility of cyclopropenylidene ligand formation. This complex has also been spectroscopically characterized by ^{1}H NMR spectroscopy, with a solution magnetic moment (μ_{eff} = 4.92 μ_B) suggesting an S = 3/2 ground state having significant unquenched orbital angular momentum.

DFT calculations support an S = 3/2 ground state. The wave function converges to a broken symmetry state in which an S = 2 iron(II) center is antiferromagnetically coupled to a cyclopropylidene radical anion (Figure S34). This electronic structure is related to those reported for other open shell iron alkylidene complexes, where multiconfigurational character is invoked.[37,38] Further support for multiconfigurational character in $PhB(^tBuIm)_3Fe(C_3H_3Ph)$ comes from CASSCF(7,6) calculations (Figures S35). The ground spin state contains two configurations with appreciable weights, which can be formulated as S = 3/2 Fe(I) bound to a singlet carbene (55%) and S = 2 Fe(II) antiferromagnetically coupled to a carbene radical (27%), respectively. The latter configuration corresponds to the broken symmetry wave function determined by DFT. This configuration transfers spin density to the carbene carbon atom, where the Löwdin spin density = −0.35 (Figure 4c). Finally, a configuration formulated as S = 3/2 Fe(III) with an alkylidene ligand makes up 6% of the weight (Figure S37).

CONCLUSIONS

In this work, we have shown the utility of the cyaphide anion as a new carbon (and phosphorus) atom source. Here, cyaphide cleavage at a 3-fold symmetric iron site provides a transient iron carbide complex whose isolation is thwarted by a rapid dimerization reaction. We anticipate that this reaction will be less likely for closed shell analogues based on other transition metal ions. Nonetheless, the carbide ligand can be trapped by styrene in the form of an alkylidene ligand, a two electron transformation that is akin to alkene epoxidation by oxo complexes.

ASSOCIATED CONTENT

Supporting Information

The Supporting Information is available free of charge at https://pubs.acs.org/doi/10.1021/jacs.4c10704.

Full experimental details, including synthetic procedures, spectra, computational information, and crystallographic data (PDF)

Optimized structures (XYZ)

Accession Codes

CCDC 2294574, 2337603−2337604, 2337607−2337608, 2368797, 2371310, and 2375405 contain the supplementary crystallographic data for this paper. These data can be obtained free of charge via www.ccdc.cam.ac.uk/data_request/cif, or by emailing data_request@ccdc.cam.ac.uk, or by contacting The Cambridge Crystallographic Data Centre, 12 Union Road, Cambridge CB2 1EZ, UK; fax: +44 1223 336033.

AUTHOR INFORMATION

Corresponding Authors

Jose M. Goicoechea − *Department of Chemistry, Indiana University, Bloomington, Indiana 47405, United States;* orcid.org/0000-0002-7311-1663; Email: jgoicoec@iu.edu

Jeremy M. Smith − *Department of Chemistry, Indiana University, Bloomington, Indiana 47405, United States;* orcid.org/0000-0002-3206-4725; Email: smith962@indiana.edu

Authors

Duleeka C. Wannipurage − *Department of Chemistry, Indiana University, Bloomington, Indiana 47405, United States*

Eric S. Yang − *Department of Chemistry, Chemistry Research Laboratory, University of Oxford, Oxford OX1 3TA, U.K.;* orcid.org/0000-0002-0851-655X

Austin D. Chivington − *Department of Chemistry, Indiana University, Bloomington, Indiana 47405, United States*

Jess Fletcher − *Department of Chemistry and Biochemistry, The Ohio State University, Columbus, Ohio 43210, United States*

Debanik Ray − *Department of Chemistry, Indiana University, Bloomington, Indiana 47405, United States*
Nobuyuki Yamamoto − *Department of Chemistry, Indiana University, Bloomington, Indiana 47405, United States*
Maren Pink − *Department of Chemistry, Indiana University, Bloomington, Indiana 47405, United States;* orcid.org/0000-0001-9049-4574

Complete contact information is available at: https://pubs.acs.org/10.1021/jacs.4c10704

Notes

The authors declare no competing financial interest.

■ ACKNOWLEDGMENTS

Funding from the NSF is gratefully acknowledged by D.C.W., A.D.C and J.M.S. (CHE-1900020 and CHE-2400199). E.S.Y. and J.M.G. thank the EPSRC and OxICFM CDT for financial support (EP/S023828/1).

■ REFERENCES

(1) (a) Fox, E. B.; Liu, Z.-W.; Liu, Z.-T. Ultraclean Fuels Production and Utilization for the Twenty-First Century: Advances toward Sustainable Transportation Fuels. *Energy Fuels* **2013**, *27*, 6335−6338. (b) Bao, J.; Yang, G.; Yoneyama, Y.; Tsubaki, N. Significant Advances in C1 Catalysis: Highly Efficient Catalysts and Catalytic Reactions. *ACS Catal.* **2019**, *9*, 3026−3053. (c) Chen, G.; Waterhouse, G. I. N.; Shi, R.; Zhao, J.; Li, Z.; Wu, L. Z.; Tung, C. H.; Zhang, T. From Solar Energy to Fuels: Recent Advances in Light-Driven C(1) Chemistry. *Angew. Chem., Int. Ed.* **2019**, *58*, 17528−17551.

(2) Rofer-DePoorter, C. K. A Comprehensive Mechanism for the Fischer−Tropsch Synthesis. *Chem. Rev.* **1981**, *81*, 447−474.

(3) Kaminsky, M. P.; Winograd, N.; Geoffroy, G. L.; Vannice, M. A. Direct SIMS Observation of Methylidyne, Methylene, and Methyl Intermediates on a Catalyst. *J. Am. Chem. Soc.* **1986**, *108*, 1315−1316.

(4) (a) Maitlis, P. Metal catalysed CO hydrogenation: hetero- or homo-, what is the difference? *J. Mol. Catal. A* **2003**, *204*−*205*, 54−61. (b) Maitlis, P. M.; Zanotti, V. The role of electrophilic species in the Fischer−Tropsch reaction. *Chem. Commun.* **2009**, 1619−1634. (c) West, N. M.; Miller, A. J. M.; Labinger, J. A.; Bercaw, J. E. Homogeneous syngas conversion. *Coord. Chem. Rev.* **2011**, *255*, 881−898.

(5) (a) Lancaster, K. M.; Roemelt, M.; Ettenhuber, P.; Hu, Y.; Ribbe, M. W.; Neese, F.; Bergmann, U.; DeBeer, S. X-ray Emission Spectroscopy Evidences a Central Carbon in the Nitrogenase Iron-Molybdenum Cofactor. *Science* **2011**, *334*, 974−976. (b) Spatzal, T.; Aksoyoglu, M.; Zhang, L.; Andrade, S. L.; Schleicher, E.; Weber, S.; Rees, D. C.; Einsle, O. Evidence for interstitial carbon in nitrogenase FeMo cofactor. *Science* **2011**, *334*, 940.

(6) (a) Rees, J. A.; Bjornsson, R.; Schlesier, J.; Sippel, D.; Einsle, O.; DeBeer, S. The Fe-V Cofactor of Vanadium Nitrogenase Contains an Interstitial Carbon Atom. *Angew. Chem., Int. Ed.* **2015**, *54*, 13249−13252. (b) Sippel, D.; Einsle, O. The structure of vanadium nitrogenase reveals an unusual bridging ligand. *Nat. Chem. Biol.* **2017**, *13*, 956−960.

(7) (a) Hu, Y.; Ribbe, M. W. Nitrogenases-A Tale of Carbon Atom(s). *Angew. Chem., Int. Ed.* **2016**, *55*, 8216−8226. (b) Sippel, D.; Rohde, M.; Netzer, J.; Trncik, C.; Gies, J.; Grunau, K.; Djurdjevic, I.; Decamps, L.; Andrade, S. L. A.; Einsle, O. A bound reaction intermediate sheds light on the mechanism of nitrogenase. *Science* **2018**, *359*, 1484−1489. (c) Kang, W.; Lee, C. C.; Jasniewski, A. J.; Ribbe, M. W.; Hu, Y. Structural evidence for a dynamic metallocofactor during N2 reduction by Mo-nitrogenase. *Science* **2020**, *368*, 1381−1385. (d) Buscagan, T. M.; Perez, K. A.; Maggiolo, A. O.; Rees, D. C.; Spatzal, T. Structural Characterization of Two CO Molecules Bound to the Nitrogenase Active Site. *Angew. Chem., Int. Ed.* **2021**, *60*, 5704−5707.

(8) Fataftah, M. S.; Mercado, B. Q.; Holland, P. L. Valence delocalization in carbon-bridged mixed-valence iron complexes. *Chem. - Eur. J.* **2023**, No. e202301962.

(9) Reinholdt, A.; Bendix, J. Transition Metal Carbide Complexes. *Chem. Rev.* **2022**, *122*, 830−902.

(10) (a) Peters, J. C.; Odom, A. L.; Cummins, C. C. A terminal molybdenum carbide prepared by methylidyne deprotonation. *Chem. Commun.* **1997**, 1995−1996. (b) Greco, J. B.; Peters, J. C.; Baker, T. A.; Davis, W. M.; Cummins, C. C.; Wu, G. Atomic Carbon as a Terminal Ligand: Studies of a Carbidomolybdenum Anion Featuring Solid-State ^{13}C NMR Data and Proton-Transfer Self-Exchange Kinetics. *J. Am. Chem. Soc.* **2001**, *123*, 5003−5013.

(11) (a) Buss, J. A.; Agapie, T. Four-electron deoxygenative reductive coupling of carbon monoxide at a single metal site. *Nature* **2016**, *529*, 72−75. (b) Buss, J. A.; Bailey, G. A.; Oppenheim, J.; VanderVelde, D. G.; Goddard, W. A., 3rd; Agapie, T. CO Coupling Chemistry of a Terminal Mo Carbide: Sequential Addition of Proton, Hydride, and CO Releases Ethenone. *J. Am. Chem. Soc.* **2019**, *141*, 15664−15674. (c) Bailey, G. A.; Agapie, T. Terminal Mo Carbide and Carbyne Reactivity: H_2 Cleavage, B−C Bond Activation, and C−C Coupling. *Organometallics* **2021**, *40*, 2881−2887.

(12) (a) Caskey, S. R.; Stewart, M. H.; Kivela, J. E.; Sootsman, J. R.; Johnson, M. J. A.; Kampf, J. W. Two Generalizable Routes to Terminal Carbido Complexes. *J. Am. Chem. Soc.* **2005**, *127*, 16750−16751. (b) Stewart, M. H.; Johnson, M. J. A.; Kampf, J. W. Terminal Carbido Complexes of Osmium: Synthesis, Structure, and Reactivity Comparison to the Ruthenium Analogues. *Organometallics* **2007**, *26*, 5102−5110.

(13) (a) Cordiner, R. L.; Hill, A. F.; Wagler, J. Facile Generation of Lithiocarbyne Complexes: $[M(\equiv CLi)(CO)_2\{HB(pzMe_2)_3\}]$ (M = Mo, W; pz = Pyrazol-1-yl). *Organometallics* **2008**, *27*, 5177−5179. (b) Colebatch, A. L.; Hill, A. F.; Shang, R.; Willis, A. C. Synthesis of a Thiocarbamoyl Alkylidyne Complex and Caveats Associated with the Use of $[Mo(\equiv CLi)(CO)_2(Tp^*)]$ (Tp* = Hydrotris(3,5-dimethylpyrazol-1-yl)borate). *Organometallics* **2010**, *29*, 6482−6487.

(14) (a) Enriquez, A. E.; White, P. S.; Templeton, J. L. Reactions of an Amphoteric Terminal Tungsten Methylidyne Complex. *J. Am. Chem. Soc.* **2001**, *123*, 4992−5002. (b) Carlson, R. G.; Gile, M. A.; Heppert, J. A.; Mason, M. H.; Powell, D. R.; Velde, D. V.; Vilain, J. M. The Metathesis-Facilitated Synthesis of Terminal Ruthenium Carbide Complexes: A Unique Carbon Atom Transfer Reaction. *J. Am. Chem. Soc.* **2002**, *124*, 1580−1581. (c) Hejl, A.; Trnka, T. M.; Day, M. W.; Grubbs, R. H. Terminal ruthenium carbido complexes as σ-donor ligands. *Chem. Commun.* **2002**, 2524−2525.

(15) (a) Kamitani, M.; Nakayasu, B.; Fujimoto, H.; Yasui, K.; Kodama, T.; Tobisu, M. Single−Carbon Atom Transfer to α,β-Unsaturated Amides from *N*-Heterocyclic Carbenes. *Science* **2023**, *379*, 484−484. (b) Koike, T.; Yu, J.-K. Ph_3PCN_2: a stable reagent for carbon atom transfer. *Science* **2024**, 305−311.

(16) (a) Agapie, T.; Diaconescu, P. L.; Cummins, C. C. Methine (CH) Transfer via a Chlorine Atom Abstraction/Benzene-Elimination Strategy: Molybdenum Methylidyne Synthesis and Elaboration to a Phosphaisocyanide Complex. *J. Am. Chem. Soc.* **2002**, *124*, 2412−2413. (b) Joost, M.; Nava, M.; Transue, W. J.; Cummins, C. C. An exploding N-isocyanide reagent formally composed of anthracene, dinitrogen and a carbon atom. *Chem. Commun.* **2017**, *53*, 11500−11503. (c) Martinez, J. L.; Lin, H. J.; Lee, W. T.; Pink, M.; Chen, C. H.; Gao, X.; Dickie, D. A.; Smith, J. M. Cyanide Ligand Assembly by Carbon Atom Transfer to an Iron Nitride. *J. Am. Chem. Soc.* **2017**, *139*, 14037−14040. (d) Kent, G. T.; Staun, S. L.; Wu, G.; Hayton, T. W. Reactivity of $[Ce(NR_2)_3]$ (R = $SiMe_3$) with Prospective Carbon Atom Transfer Reagents. *Organometallics* **2020**, *39*, 2375−2382. (e) Le, L. N. V.; Bailey, G. A.; Scott, A. G.; Agapie, T. Partial synthetic models of FeMoco with sulfide and carbyne ligands: Effect of interstitial atom in nitrogenase active site. *Proc. Natl. Acad. Sci. U.S.A.* **2021**, *118*, No. e2109241118. (f) Nguyen, T. H.; Yu, X.; Kent, G. T.; Autschbach, J.; Hayton, T. W. U−C Bond Insertion, Ring-Opening, and C−H Activation in a Uranium Bis(diisopropylamino)-

cyclopropenylidene (BAC) Adduct. *Organometallics* **2023**, *42*, 1005−1012.
(17) Gary, J. B.; Buda, C.; Johnson, M. J. A.; Dunietz, B. D. Accessing Metal-Carbide Chemistry. A Computational Analysis of Thermodynamic Considerations. *Organometallics* **2008**, *27*, 814−826.
(18) (a) Lee, Y.; Peters, J. C. Silylation of iron-bound carbon monoxide affords a terminal Fe carbyne. *J. Am. Chem. Soc.* **2011**, *133*, 4438−4446. (b) Deegan, M. M.; Peters, J. C. Synthesis and Functionalization Reactivity of Fe-Thiocarbonyl and Thiocarbyne Complexes. *Polyhedron* **2021**, *209*, No. 115461.
(19) Görlich, T.; Coburger, P.; Yang, E. S.; Goicoechea, J. M.; Grützmacher, H.; Müller, C. The Chemistry of the Cyaphide Ion. *Angew. Chem., Int. Ed.* **2023**, *62*, No. e202217749.
(20) Smith, J. M.; Subedi, D. The structure and reactivity of iron nitride complexes. *Dalton Trans.* **2012**, *41*, 1423−1429.
(21) Valdez-Moreira, J. A.; Beagan, D. M.; Yang, H.; Telser, J.; Hoffman, B. M.; Pink, M.; Carta, V.; Smith, J. M. Hydrocarbon Oxidation by an Exposed, Multiply Bonded Iron(III) Oxo Complex. *ACS Cent. Sci.* **2021**, *7*, 1751−1755.
(22) Valdez-Moreira, J. A.; Wannipurage, D. C.; Pink, M.; Carta, V.; Moënne-Loccoz, P.; Telser, J.; Smith, J. M. Hydrogen atom abstraction by a high-spin [Fe^{III}=S] complex. *Chem.* **2023**, *9*, 2601−2609.
(23) Valdez-Moreira, J. A.; Thorarinsdottir, A. E.; DeGayner, J. A.; Lutz, S. A.; Chen, C. H.; Losovyj, Y.; Pink, M.; Harris, T. D.; Smith, J. M. Strong π-Backbonding Enables Record Magnetic Exchange Coupling Through Cyanide. *J. Am. Chem. Soc.* **2019**, *141*, 17092−17097.
(24) (a) Wilson, D. W. N.; Urwin, S. J.; Yang, E. S.; Goicoechea, J. M. A Cyaphide Transfer Reagent. *J. Am. Chem. Soc.* **2021**, *143*, 10367−10373. (b) Cordaro, J. G.; Stein, D.; Ruegger, H.; Grutzmacher, H. Making the true ″CP″ ligand. *Angew. Chem., Int. Ed.* **2006**, *45*, 6159−6162. (c) Trathen, N.; Leech, M. C.; Crossley, I. R.; Greenacre, V. K.; Roe, S. M. Synthesis and electronic structure of the first cyaphide-alkynyl complexes. *Dalton Trans.* **2014**, *43*, 9004−9007. (d) Furfari, S. K.; Leech, M. C.; Trathen, N.; Levis, M. C.; Crossley, I. R. Cyaphide-alkynyl complexes: metal-ligand conjugation and the influence of remote substituents. *Dalton Trans.* **2019**, *48*, 8131−8143. (e) Levis, M. C.; Pearce, K. G.; Crossley, I. R. Controlled Reactivity of Terminal Cyaphide Complexes: Isolation of the 5-Coordinate [$Ru(dppe)_2(C{\equiv}P)$]. *Inorg. Chem.* **2019**, *58*, 14800−14807. (f) Görlich, T.; Frost, D. S.; Boback, N.; Coles, N. T.; Dittrich, B.; Müller, P.; Jones, W. D.; Müller, C. Photochemical C(sp)-C(sp^2) Bond Activation in Phosphaalkynes: A New Route to Reactive Terminal Cyaphido Complexes L_nM-C≡P. *J. Am. Chem. Soc.* **2021**, *143*, 19365−19373. (g) Levis, M. C.; Helm, M. L.; Turner, J. F. C.; Crossley, I. R. A Monomeric Bis(cyaphido) Complex. *Chem - Eur. J.* **2024**, No. e202303370.
(25) Hoerger, C. J.; Heinemann, F. W.; Louyriac, E.; Maron, L.; Grützmacher, H.; Meyer, K. Formation of a Uranium-Bound η^1-Cyaphide (CP^-) Ligand via Activation and C−O Bond Cleavage of Phosphaethynolate (OCP^-). *Organometallics* **2017**, *36*, 4351−4354.
(26) Scepaniak, J. J.; Harris, T. D.; Vogel, C. S.; Sutter, J.; Meyer, K.; Smith, J. M. Spin Crossover in a Four-Coordinate Iron(II) Complex. *J. Am. Chem. Soc.* **2011**, *133*, 3824−3827.
(27) (a) Cummins, C. C. Reductive cleavage and related reactions leading to molybdenum−element multiple bonds: new pathways offered by three-coordinate molybdenum(III). *Chem. Commun.* **1998**, 1777−1785. (b) Laplaza, C. E.; Odom, A. L.; Davis, W. M.; Cummins, C. C.; Protasiewicz, J. D. Cleavage of the Nitrous Oxide NN Bond by a Tris(amido)molybdenum(III) Complex. *J. Am. Chem. Soc.* **1995**, *117*, 4999−5000.
(28) Laplaza, C. E.; Davis, W. M.; Cummins, C. C. A Molybdenum−Phosphorus Triple Bond: Synthesis, Structure, and Reactivity of the Terminal Phosphido (P^{3-}) Complex [$Mo(P)(NRAr)_3$]. *Angew. Chem., Int. Ed.* **1995**, *34*, 2042−2044.
(29) The diiron μ_2-ethynediyl complex $PhB(^tBuIm)_3Fe$-C≡C-$Fe(^tBuIm)_3BPh$ can also be prepared by reaction of $PhB(tBuIm)_3Fe$-C≡CH and $PhB(tBuIm)_3FeNH^tBu$, see Supporting Information for more details.
(30) (a) Goedken, V. L.; Deakin, M. R.; Bottomley, L. A. Molecular Stereochemistry of a Carbon-bridged Metalloporphyrin: y-Carbido-bis(5,10,'15,20-tetraphenylporphinatoiron). *J. Chem. Soc. Chem. Commun.* **1982**, *0*, 607−608. (b) Kienast, A.; Galich, L.; Murray, K. S.; Moubaraki, B.; Lazarev, G.; Cashion, J. D.; Homborg, H. μ-Carbido Diporphyrinates and Diphthalocyaninates of Iron and Ruthenium. *J. Porphyrins Phthalocyanines* **1997**, *1*, 141−157. (c) Galich, L.; Kienast, A.; Hückstädt, H.; Homborg, H. Synthesen, spektroskopische Eigenschaften und Kristallstrukturenzweikerniger homo- und heteroleptischerl-Carbido-Komplexevon Eisen(IV) mit Phthalocyaninat- und Tetraphenylporphyrinat-Liganden. *Z. Anorg. Allg. Chem.* **1998**, *624*, 1235−1242. (d) Colomban, C.; Kudrik, E.; Tyurin, D.; Albrieux, F.; Nefedov, S.; Afanasiev, P.; Sorokin, A. Synthesis and characterization of μ-nitrido, μ-carbido and μ-oxo dimers of iron octapropylporphyrazine. *Dalton Trans.* **2015**, *44*, 2240−2251.
(31) (a) Scepaniak, J. J.; Vogel, C. S.; Khusniyarov, M. M.; Heinemann, F. W.; Meyer, K.; Smith, J. M. Synthesis, Structure, and Reactivity of an Iron(V) Nitride. *Science* **2011**, *331*, 1049−1052. (b) Cutsail, G. E., III; Stein, B. W.; Subedi, D.; Smith, J. M.; Kirk, M. L.; Hoffman, B. M. EPR, ENDOR and Electronic Structure Studies of the Jahn-Teller Distortion in an Fe^V Nitride. *J. Am. Chem. Soc.* **2014**, *136*, 12323−12336.
(32) Glendening, E. D.; Landis, C. R.; Weinhold, F. Natural bond orbital methods. *WIREs Comp. Mol. Sci.* **2012**, *2*, 1−42.
(33) Bailey, G. A.; Buss, J. A.; Oyala, P. H.; Agapie, T. Terminal, Open-Shell Mo Carbide and Carbyne Complexes: Spin Delocalization and Ligand Noninnocence. *J. Am. Chem. Soc.* **2021**, *143*, 13091−13102.
(34) Valdez-Moreira, J. A.; Thorarinsdottir, A. E.; DeGayner, J. A.; Lutz, S. A.; Chen, C. H.; Losovyj, Y.; Pink, M.; Harris, T. D.; Smith, J. M. Strong π-Backbonding Enables Record Magnetic Exchange Coupling Through Cyanide. *J. Am. Chem. Soc.* **2019**, *141*, 17092−17097.
(35) (a) Laplaza, C. E.; Johnson, M. J. A.; Peters, J. C.; Odom, A. L.; Kim, E.; Cummins, C. C.; George, G. N.; Pickering, I. J. Dinitrogen Cleavage by Three-Coordinate Molybdenum(III) Complexes: Mechanistic and Structural Data. *J. Am. Chem. Soc.* **1996**, *118*, 8623−8638. (b) Curley, J. J.; Cook, T. R.; Reece, S. Y.; Muller, P.; Cummins, C. C. Shining Light on Dinitrogen Cleavage: Structural Features, Redox Chemistry, and Photochemistry of the Key Intermediate Bridging Dinitrogen Complex. *J. Am. Chem. Soc.* **2008**, *130*, 9394−9405.
(36) (a) Giusti, M.; Solari, E.; Giannini, L.; Floriani, C.; Chiesi-Villa, A.; Rizzoli, C. Iron-Carbene Bonded to a Planar Tetraoxo Surface Defined by Dimethoxy-*p*-*tert*-butylcalix[4]arene Dianion. *Organometallics* **1997**, *16*, 5610−5612. (b) Esposito, V.; Solari, E.; Floriani, C.; Re, N.; Rizzoli, C.; Chiesi-Villa, A. Binding and Redox Properties of Iron(II) Bonded to an Oxo Surface Modeled by Calix[4]arene. *Inorg. Chem.* **2000**, *39*, 2604−2613.
(37) Russell, S. K.; Hoyt, J. M.; Bart, S. C.; Milsmann, C.; Stieber, S. C. E.; Semproni, S. P.; DeBeer, S.; Chirik, P. J. Synthesis, Electronic Structure and Reactivity of Bis(imino)pyridine Iron Carbene Complexes: evidence for a Carbene Radical. *Chem. Sci.* **2014**, *5*, 1168−1174.
(38) Hakey, B. M.; Leary, D. C.; Xiong, J.; Harris, C. F.; Darmon, J. M.; Petersen, J. L.; Berry, J. F.; Guo, Y.; Milsmann, C. High Magnetic Anisotropy of a Square-Planar Iron-Carbene Complex. *Inorg. Chem.* **2021**, *60*, 18575−18588.

https://doi.org/10.1021/jacs.4c10704
J. Am. Chem. Soc. 2024, 146, 27173−27178